Thyrotropin-releasing-hormone-synthesizing neurons of the hypothalamic paraventricular nucleus are inhibited by glycinergic inputs

Edina Varga[1*], Erzsébet Farkas[1*], Györgyi Zséli[1], Andrea Kádár[1], Alexandra Venczel[1], Dóra Kővári[1], Dorottya Németh[1], Zoltán Máté[2], Ferenc Erdélyi[2], András Horváth[3,4], Ottó Szenci[3,4], Masahiko Watanabe[5], Ronald M. Lechan[6,7], Balázs Gereben[1] and Csaba Fekete[1,6]

[1]Department of Endocrine Neurobiology, Institute of Experimental Medicine, Hungarian Academy of Sciences, Budapest, Hungary H-1083

[2]Medical Gene Technology Unit, Institute of Experimental Medicine, Hungarian Academy of Sciences, Budapest, Hungary H-1083

[3]Department and Clinic for Production Animals, University of Veterinary Medicine Budapest, Üllő, Dóra Major, Hungary, H-2225

[4]MTA–SZIE Large Animal Clinical Research Group, Üllő, Dóra major, Hungary, H-2225

[5]Department of Anatomy, Hokkaido University School of Medicine, Sapporo 060-8638, Japan

[6]Department of Medicine, Division of Endocrinology, Diabetes and Metabolism, Tupper Research Institute, Tufts Medical Center, Boston, MA, USA 02111.

[7]Department of Neuroscience, Tufts University School of Medicine, Boston, MA, USA 02111.

[*]Contributed equally to the work

Running title: Glycinergic innervation of TRH neurons in the PVN

Keywords: Hypophysiotropic TRH neurons, hypothalamic paraventricular nucleus, innervation, glycine, patch-clamp electrophysiology

Corresponding author: Csaba Fekete MD PhD fekete.csaba@koki.mta.hu

Abstract

Background: Glycine is a classical neurotransmitter that has role in both inhibitory and excitatory synapses. To understand whether glycinergic inputs are involved in the regulation of the hypophysiotropic thyrotropin-releasing hormone (TRH) neurons, the central controllers of the hypothalamic-pituitary-thyroid (HPT) axis, the glycinergic innervation of the TRH neurons was studied in the hypothalamic paraventricular nucleus (PVN).

Methods: Double-labeling immunocytochemistry and patch clamp electrophysiology was used to determine the role of the glycinergic neurons in the regulation of TRH neurons in the PVN. Anterograde- and retrograde tracing methods were used to determine the sources of the glycinergic input of TRH neurons.

Results: Glycine transporter 2 (GLYT2), a marker of glycinergic neurons, containing axons was found to establish symmetric type of synapses on TRH neurons in the PVN. Furthermore, glycine receptor-immunoreactivity was observed in these TRH neurons. The raphe magnus (RMg) and the ventrolateral periaqueductal gray (VLPAG) were found to be the exclusive sources of the glycinergic innervation of the TRH neurons within the PVN.

Patch-clamp electrophysiology using sections of TRH-IRES-tdTomato mice showed that glycine hyperpolarized the TRH neurons and completely blocked the firing of these neurons. Glycine also markedly hyperpolarized the TRH neurons in the presence of tetrodotoxin demonstrating the direct effect of glycine. In more than 60% of the TRH neurons, spontaneous inhibitory postsynaptic currents (sIPSC) were observed, even after the pharmacological inhibition of glutamatergic and GABAergic neuronal transmission. The glycine antagonist, strychnine, almost completely abolished these sIPSCs, demonstrating the inhibitory nature of the glycinergic input of TRH neurons.

Conclusions: These data demonstrate that TRH neurons in the PVN receive glycinergic inputs from the RMg and the VLPAG. The symmetric type of synaptic connection and the results of the electrophysiological experiments demonstrate the inhibitory nature of these inputs.

INTRODUCTION

Glycine is a classical neurotransmitter that has an important role in both inhibitory and excitatory synapses (1). Glycinergic neurons are primarily located in the brainstem and spinal cord (2), however, glycinergic axons are also observed in the hypothalamus (3). Two glycine-transporter subtypes (GlyT) were identified in the central nervous system: glycine transporter-1 (GlyT1), mainly located in glial cells and nerve terminals of excitatory neurons, and glycine transporter-2 (GlyT2), present exclusively in glycinergic neurons (4, 5).

Glycine is released from inhibitory, presynaptic terminals and binds to strychnine-sensitive glycine receptors that are located in the postsynaptic membrane of target cells (1). Activation of glycine receptors leads to influx of chloride ions into the cytoplasm and thereby, inhibits the postsynaptic neuron (6). In addition, glycine is also important for excitatory glutamatergic neurotransmission because it serves as an essential co-agonist of glutamate at NMDA receptors (7).

The hypothalamic paraventricular nucleus (PVN), where hypophysiotropic thyrotropin-releasing hormone- (TRH)-synthesizing neurons, the main central regulators of the hypothalamic-pituitary-thyroid (HPT) axis reside(8), is densely innervated by glycinergic axons (3). Within the PVN, glycine has been shown to elicit large, inward currents (9). Furthermore, evoked glycinergic currents can be observed in parvocellular PVN neurons in the presence of the blockers of glutamate and GABA receptors (9), suggesting that ascending glycinergic pathways regulate parvocellular neurons in the PVN.

Based on these data, we hypothesized that glycinergic brainstem neurons are involved in the regulation of the TRH neurons in the PVN including the hypophysiotropic TRH neurons. To test this hypothesis, we performed neuroanatomical and electrophysiological experiments. Since TRH neurons are dispersed in the PVN, identification of these cells was difficult in electrophysiological studies. In addition, in morphological studies, the cell bodies of TRH

neurons could only be identified after inhibition of axonal transport by colchicine treatment. Therefore, to facilitate both the electrophysiological and morphological studies, we generated a TRH-IRES-tdTomato knock in mouse line in which the TRH neurons can be easily identified based on the presence of the red fluorescent protein in their perikarya.

Materials and methods

Animals

The experiments were carried out in adult, male, CD1 mice (N=8), GlyT2::GFP mice (N=9) (3), TRH-IRES-tdTomato mice (N=30), double transgenic mice heterozygous for TRH-IRES-tdTomato and GlyT2::Cre (10) (TRH-IRES-tdTomato//GlyT2::Cre; N=10), and, weighing 30–40 g, housed under standard environmental conditions (light between 06:00 and 18:00 h, temperature 22±1ºC, rat chow and water *ad libitum*). The *in vitro* patch clamp electrophysiology studies were performed on mice between P40 and P60 days of age. All experimental protocols were reviewed and approved by the Animal Welfare Committee at the Institute of Experimental Medicine of the Hungarian Academy of Sciences.

Generation of the TRH-IRES-tdTomato mouse line

An IRES tdTomato cassette was inserted into the mouse TRH locus using CRISPR/Cas9 (11) on FVB.129P2-Pde6b^{+} Tyr$^{c\text{-}ch/}$AntJ (FVB/Ant) background. The 1473 bp long 5' and the 1375bp long 3' TRH arms were obtained by PCR on FVB/Ant gDNA (5' TRH arm sense oligonucleotide: ccgctcgagCACCTTGGCACCCTGATACCAGGAA; antisense: tccccgcggTTACTCCTCC AGAGGTTCCCTGA; 3' TRH arm sense: ataagaatgcggccgc*t*GGTTAGAGTCAGGCTTT AGGTCTA; antisense: ctagctagc CTGGCATGGTGACTCATCTATAACAT). The 5' arm was cloned between XhoI and SacII followed by IRES of the pPRIG vector (12) between SacII and EcoRI and the tdTomato coding region between EcoRI and NotI sites. The 3' arm was placed between NotI and NheI. The construct was assembled in a D10 vector and confirmed by sequencing.

Pronuclear microinjection was carried out on fertilized eggs of FVB/Ant mice, using of a single guide RNA with the target sequence of GGAGTAAGGTTAGAGTC and Cas9 mRNA (Trilink).

Founders were identified with qPCR for tdTomato (tdTomF GCTCCAAGGCGTACGTGAA, tdTomR GGAAGGACAGCTTCTTGTAATCG, tdTom_probe 6-FAM-CACCCCGCCGACAT-MGBNFQ) followed by checking the insertion sites with outer and inner PCR oligos (CTTCCATGAGAGGAGTATTTATCA, CATGGACGAGCTGTACAAGTA, GGCCGCTATGACTTTAGCTTC, CTTACACCCACTGCCTTTGAC and GTAGTCAGGCACGTCGTATGG). A founder with a single copy of the targeting cassette was selected for breeding.

Heterozygote F1 animals were crossbred with littermate animals of identical genotype. Mice were bred and maintained as homozygous colonies.

Characterization of the TRH-IRES-tdTomato mice

All solutions were made with MilliQ water treated with diethylpyrocarbonate (DEPC, 0.2µl/ml) overnight and then autoclaved. TRH-IRES-tdTOMATO mice (N=6) were deeply anesthetized with ketamine/xylazine (ketamine 50 mg/kg, xylazine 10 mg/kg body weight, ip) and the animals perfused transcardially with 10 ml 0.01 M PBS, pH 7.4, followed by 50 ml of 4% PFA in 0.1 M PB, pH 7.4. The brains were quickly removed, postfixed by immersion in the same fixative for 2 hours at RT, cryoprotected in 20% sucrose in PBS at 4°C overnight and then frozen using powdered dry ice. Serial 20-µm-thick coronal sections through the whole brain were cut on a cryostat (Leica Microsystems, Wetzlar, Germany), collected in freezing solution and stored at −20°C until used.

The digoxigenin-labeled antisense mouse pro-TRH cRNA probe was synthesized using a 741-base (corresponding to the 106–846 nucleotides of the mouse TRH mRNA; BC053493) cDNA template (13) as described earlier (14). The hybridization was performed in 200 µl polypropylene tubes in a hybridization buffer (50% formamide, 2× SSC, 10% dextran sulfate, 0.5% SDS, 250 µg/ml denatured salmon sperm DNA) containing the digoxigenin-labeled probe

(1:100 dilution) for 16 hr at 56°C. The sections were washed in 1× SSC for 15 min and then treated with RNase (25 μg/ml) for 1 hr at 37°C. After additional washes in 0.1× SSC (four times for 15 min each) at 65°C, sections were washed in PBS, treated with the mixture of 0.5% Triton X-100 and 0.5% H_2O_2 for 15 min, and then with 2% BSA in PBS for 20 min to reduce the nonspecific antibody binding. The sections were incubated with a mixture of sheep anti-digoxigenin-peroxidase Fab fragments (1:100; Boehringer Mannheim) and rabbit anti-RFP serum (Rockland Immunochemicals Inc., Limerick, PA, USA, Indianapolis, IN, USA) diluted at 1:3000 in 1% BSA in PBS for 2 d at 4°C. The sections were rinsed in PBS and then the in situ hybridization signal was amplified using the TSA amplification kit according to the manufacturer's instructions. After further washes, the sections were incubated in a mixture of Fluorescein DTAF-conjugated Streptavidin (1:300, Jackson Immunoresearch Labs, West Grove, PA, USA) and Alexa 555-conjugated donkey anti-rabbit IgG (1:500, Jackson Immunoresearch Labs, West Grove, PA) for 2 hours and mounted glass slides. Slides were air dried and coverslipped with Vectashield mounting medium (Vector Laboratories Inc, Burlingame, CA, USA). Images were taken with a Zeiss LSM 780 laser scanning confocal microscope.

Generation of a sheep antibody against tdTomato

The tdTomato coding region was inserted into a pET26b (+) vector (Merck, Darmstadt, Germany) by adding a C-terminal His-tag. Recombinant expression of His-tagged tdTomato was performed in Rosetta 2(DE3) E. Coli strain (Merck, Darmstadt, Germany). Induction was performed at 18 °C with 0.5 mM IPTG and the recombinant protein was expressed overnight. The cells were harvested by centrifugation at 4000xg for 30 min at 4 °C and the pellet was stored at -20 °C then resuspended in 20 ml lysis buffer (50 mM Tris base, 0.2 M NaCl, 5 % glycerin, 1 mM DTT, 1 mM TCEP, 1 mM PMSF supplemented with Roche Complete, Mini,

EDTA-free Protease Inhibitor Cocktail, pH 7.5) followed by lysis with 500 µg/ml lysozyme at 4 °C for 4 h and further incubation with 5 mM $MgCl_2$ and 1 mg/ml DNase. The His-tagged tdTomato was purified on 3 ml Ni-NTA column (ThermoFisher, Waltham, MA, USA) equilibrated with column buffer (20 mM Tris base, 200 mM NaCl, pH 7.5). After washing the column with 75 mM imidazole containing column buffer pure tdTomato fraction was eluted with 500 mM imidazole column buffer at pH 7.5. The eluted fraction was analyzed by SDS-PAGE and dialyzed against 0.1M PBS.

760 µg tdTomato in 1 ml PBS was emulsified with an equal volume of Freund's complete adjuvant (Sigma-Aldrich, St. Louis, MO, USA) and injected subcutaneously into sheep. Subsequent boosts with Freund's incomplete adjuvant were administered at 28-day intervals. Eight days after the fourth immunization, blood was collected and the serum was separated by centrifugation.

Animal preparation for examination of the glycinergic input to TRH neurons in the PVN

CD1 mice (N=8) were deeply anesthetized with ketamine/xylazine (ketamine 50 mg/kg, xylazine 10 mg/kg body weight, intraperitoneal (ip)) and the animals perfused transcardially with 10 ml 0.01 M phosphate-buffered saline (PBS), pH 7.4, followed sequentially by 50 ml of 2% paraformaldehyde (PFA) / 4% acrolein in 0.1 M phosphate buffer (PB), pH 7.4, and then by 20 ml of 2% PFA in the same buffer. The brains were rapidly removed and stored in 4% PFA for 2 h for light microscopy (N=4) at room temperature (RT), or 24 h for electron microscopy (N=4) at 4^{o}C.

Sectioning and section pretreatment for light microscopic studies

The brains were cryoprotected in 30% sucrose in PBS at 4^{o}C overnight, then frozen using powdered dry ice. Serial, 25 µm thick coronal sections through the PVN were cut on a freezing

185 microtome (Leica Microsystems, Wetzlar, Germany), collected in cryoprotectant solution (30%
186 ethylene glycol; 25% glycerol; 0.05 M PB) and stored at -20°C until used. Series of sections
187 from each brain were treated with 1% sodium borohydride (Sigma-Aldrich, St. Louis, MO,
188 USA) in distilled water (DW) for 30 min and with a mixture of 0.5% Triton X-100 and 0.5%
189 H_2O_2 in PBS for 15 min. To reduce nonspecific antibody binding, the sections were treated with
190 2% normal horse serum (NHS) in PBS for 20 min.
191
192 *Double-labeling immunofluorescence for examination of the glycinergic input of TRH neurons*
193 *in the PVN*
194 Pretreated sections of CD1 mice were incubated in a mixture of rabbit anti-GlyT2 IgG (15, 16)
195 and sheep anti-TRH IgG (1:4000) (17) in PBS containing 2% NHS and 0.2% sodium-azide
196 (antiserum diluent) for 2 days at 4°C. After rinses in PBS, the sections were incubated in a
197 mixture of Alexa 555-conjugated donkey anti-rabbit IgG (1:500, Jackson Immunoresearch Labs,
198 West Grove, PA, USA) and Alexa 488-conjugated donkey anti-sheep IgG (1:500, Jackson
199 Immunoresearch Labs, West Grove, PA, USA) in antiserum diluent. After rinses in PBS, the
200 sections were mounted onto glass slides, and coverslipped with Vectashield mounting medium
201 (Vector Laboratories Inc, Burlingame, CA, USA).
202
203 *Double labeling immuno- electron microscopy for examination of the glycinergic input of TRH*
204 *neurons in the PVN*
205 Serial, 25µm thick coronal sections were cut on a Leica VT 1000S vibratome (Leica
206 Microsystems, Wetzlar, Germany) through the rostro-caudal extent of the PVN and collected
207 in PBS. The sections were treated with 1% sodium borohydride (Sigma-Aldrich, St. Louis, MO,
208 USA) in 0.1 M PB for 30 min, followed by 0.5% H_2O_2 in PBS for 15 min. The sections were
209 cryoprotected in 15% sucrose in PBS for 15 min at RT and in 30% sucrose in PBS overnight at

4°C and then, quickly frozen over liquid nitrogen and thawed at RT. This freezing-thawing cycle was repeated 3 times to improve antibody penetration. To reduce the nonspecific antibody binding, the sections were treated with 2% NHS in PBS for 20 min. Sections were placed into a mixture of rabbit anti-GlyT2 IgG (1µg/ml) and sheep anti-TRH IgG (1:1000) for 4 days at 4°C. After rinsing in PBS and in a mixture of 0.1% cold water fish gelatin (Aurion, Wageningen, Netherlands) and 1% BSA (Sigma-Aldrich, St. Louis, MO, USA) in PBS, the sections were incubated in a cocktail of donkey anti-sheep IgG-conjugated with 0.8 nm colloidal gold (1:100, Electron Microscopy Sciences, Fort Washington, PA, USA) and biotinylated donkey anti-rabbit IgG (1:500, Jackson Immunoresearch Labs, West Grove, PA, USA) in the same cold water fish gelatin- and BSA-containing solution for 20 h at 4°C. After washing in PBS, the sections were fixed in 1.25% glutaraldehyde (Electron Microscopy Sciences, Fort Washington, PA, USA) in 0.1M PB for 10 min. The gold particles were silver intensified with the Aurion R-Gent SE-LM Kit (Aurion, Wageningen, Netherlands) (18). After rinsing in 0.2M sodium citrate, pH 7.5, the sections were immersed in ABC Elite Complex (1:1000, Vector Laboratories Inc, Burlingame, CA, USA) diluted in 0.05M TRIS buffer for 1 hour at RT. The GlyT2 immunoreactivity was detected with NiDAB developer (0.025% DAB/0.0036% H_2O_2 in 0.05 M Tris buffer, pH 7.6). The sections were osmicated, and then treated with 2% uranyl acetate in 70% ethanol for 30 min. Following dehydration in an ascending series of ethanol and acetonitrile, the sections were flat embedded in Durcupan ACM epoxy resin (Fluka, Sigma-Aldrich, St. Louis, MO, USA) on liquid release agent (Electron Microscopy Sciences, Fort Washington, PA, USA)-coated slides, and polymerized at 56 °C for 2 days. Ultrathin 50–60 nm sections were cut with Leica ultracut UCT ultramicrotome (Leica Microsystems, Wetzlar, Germany), collected onto Formvar-coated, single slot grids, and examined with a JEOL electron microscope (Jeol, Tokyo, Japan).

Tissue preparation for the examination of the glycine receptor (GlyR) content of TRH neurons in the PVN

TRH-IRES-tdTomato mice (N=5) were deeply anesthetized with ketamine/xylazine (ketamine 50 mg/kg, xylazine 10 mg/kg body weight, ip) and perfused transcardially with 10 ml 0.01 M PBS, pH 7.4, followed by 50 ml of 4% PFA in 0.1 M PB, pH 7.4. The brains were rapidly removed, postfixed in 4% PFA for 2 hours at RT and cryoprotected in 30% sucrose in 0.01 M PBS overnight at room temperature. The brains were then frozen with powdered dry ice and stored at -20^{o}C until use.

Serial, 25 µm thick coronal sections through the PVN were cut on a freezing microtome, collected in cryoprotectant solution and stored at -20^{o}C until use.

Series of sections from each brain were subjected to pepsin pretreatment to facilitate antigen exposure (16). The sections were incubated in 1 mg/ml pepsin (Dako Agilent, Santa Clara, CA, USA) for 7 min at 37 °C. After washing in PBS, the sections were treated with 0.5% Triton X-100/0.5% H_2O_2 in PBS for 15 min, immersed in 2% NHS in PBS for 20 min and then incubated in a mixture of guinea pig-GlyRa IgG (15) (16) and rabbit-RFP antiserum (1:3000, Rockland Immunochemicals Inc., Limerick, PA, USA) in antiserum diluent for 2 days at 4^{o}C. After rinses in PBS, the sections were incubated in biotinylated donkey anti-guinea pig IgG (1:500, Jackson Immunoresearch Labs, West Grove, PA, USA) for two hours and in ABC Elite Complex (1:1000, Vector Laboratories Inc, Burlingame, CA, USA) in 0.05M TRIS buffer for an hour. The immunoreaction was amplified with biotinylated tyramide using the TSA amplification kit (Perkin Elmer Life and Analytical Sciences, Waltham, MA, USA). After further washes, the sections were incubated in a mixture of the Fluorescein DTAF-conjugated Streptavidin (1:300, Jackson Immunoresearch Labs, West Grove, PA, USA) and Alexa 555-conjucated donkey anti-rabbit IgG (1:500, Jackson Immunoresearch Labs, West Grove, PA, USA), mounted onto glass

slides and coverslipped with Vectashield mounting medium (Vector Laboratories Inc, Burlingame, CA, USA).

Retrograde tract-tracing and tissue preparation for the identification of the sources of the glycinergic innervation of the PVN

The retrograde tracer, cholera toxin β subunit (CTB; List Biological Labs, Campbell, CA, USA), was injected by iontophoresis into the PVN of GlyT2/GFP mice (N=9). The animals were anesthetized ip with ketamine-xylazine (ketamine: 50 mg/kg; xylazine: 10 mg/kg body weight) and their head positioned in a stereotaxic apparatus with the Bregma and Lambda in the horizontal plane. Through a burr hole in the skull, a glass micropipette (17.5-20 μm outer tip diameter) filled with 0.5% CTB in 0.01M PB at pH 8.0 was lowered into the brain at stereotaxic coordinates corresponding to the PVN (anterior–posterior, -0.9 mm from the Bregma; lateral, -0.15 mm; and dorsoventral, -4.8 mm from the surface of the skull), based on the atlas of Paxinos and Watson (19). CTB was deposited over 3 min of positive current (4 μA, pulsed on—off at 7s intervals) using a constant-current source (Stoelting, Wood Dale, IL, USA). The animals were anesthetized 7–10 days after tracer deposition and perfused with 10 ml PBS, pH 7.4, followed by 50 ml of 4% paraformaldehyde in 0.1 M PB, pH 7.4. The brains were rapidly removed, postfixed in 4% PFA for 2 hours at RT, cryoprotected in 30% sucrose in PBS overnight at RT, then frozen using powdered dry ice and stored at -20^{o}C until use. Twenty-five-μm-thick coronal sections were cut on a freezing microtome into one-in-four series of sections.

Immunohistochemically identification of the CTB injection sites

Series of sections was pre-treated as described above and then incubated in goat anti-CTB serum (1:10000, List Biological Labs, Campbell, CA, USA) for 2 days. Following washes in

PBS, the sections were immersed in biotinylated donkey anti-sheep IgG (1:500, Jackson Immunoresearch Labs, West Grove, PA, USA) for 2 h and in ABC (1:1000, ABC Elite, Vector Laboratories Inc, Burlingame, CA, USA) diluted in 0.05M Tris buffer for one hour. Following rinses in PBS, peroxidase activity was visualized with NiDAB developer. The sections were mounted on gelatin coated slides, air dried, counterstained with 1% cresyl-violet and coverslipped with DPX mounting medium (Sigma-Aldrich, St. Louis, MO, USA).

Double-labeling immunofluorescence for the identification of the sources of the glycinergic input of the PVN

One of the four series of sections was pre-treated as described above and incubated in a mixture of goat anti-CTB serum (1:5000, List Biological Labs, Campbell, CA, USA) and rabbit anti-GFP serum (1:0,000, Life technologies) for 2 days at 4°C. Then, the sections were immersed in biotinylated donkey anti-sheep IgG (1:500, Jackson Immunoresearch Labs, West Grove, PA, USA) for 2 h, followed by ABC (1:1000, ABC Elite, Vector Laboratories Inc, Burlingame, CA, USA) for 2 hours. The immunoreaction product was amplified with TSA amplification kit for 10 min. The signals were visualized by incubation in a mixture of Alexa 488-conjugated donkey anti-rabbit IgG (1:500, Jackson Immunoresearch Labs, West Grove, PA, USA) and Alexa 555-conjugated Streptavidin (1:500, Jackson Immunoresearch Labs, West Grove, PA, USA) for two hours, mounted onto glass slides and coverslipped with Vectashield mounting medium (Vector Laboratories Inc, Burlingame, CA, USA).

Virus injection and tissue preparation for the identification of the sources of the glycinergic innervation of the TRH neurons in the PVN

As our retrograde tract-tracing experiment showed that the VLPAG and the RMg are the sources of the glycinergic input of the PVN, *DIO-hChR2(H134R)-eYFP adeno-associated virus*

(AAV) was injected to the VLPAG (N=5) or RMg (N=5) in *TRH-IRES-tdTomato//GlyT2-Cre* mice. The Cre expression in the GLYT2 cells allowed the glycinergic neuron specific expression of the hChR2(H134R)-eYFP fusion protein, while the tdTomato expression of TRH neurons facilitated the detection of TRH neurons. The surgeries were performed in a BSL-2 AAV facility. The mice were anesthetized ip with ketamine-xylazine (ketamine: 50 mg/kg; xylazine: 10 mg/kg body weight) and their head positioned in a stereotaxic apparatus with the Bregma and Lambda in the horizontal plane. Through a burr hole in the skull, a glass pipette (25-µm tip) connected to a Nanoject II/Nanoliter 2000 microinjector (WPI Inc., Sarasota, FL, USA) was lowered into the brain at stereotaxic coordinates corresponding to the VLPAG (anteroposterior: -4.72 mm, mediolateral: -0.4 mm, dorsoventral: -2.75 mm), or RMg (anteroposterior: -5.34 mm, mediolateral: 0 mm, dorsoventral: -5.7mm) based on the atlas of Paxinos and Watson (19). 80 nl (RMg) and 150 nl (VLPAG) of virus-containing solution (4.5 $x10^{12}$ virus/ml, titer: 1x10^13 GC/ml) was injected unilaterally into the nuclei at a rate of 5nl/sec. Five minutes after the injection, the pipette was slowly removed, the scalp sutured and the mice housed in BSL-2 quarantine for 2 weeks before experimentation. The animals were re-anaesthetized and perfused transcardially with 10 ml 0.01 M PBS, pH 7.4, followed by 50 ml of 4% PFA in 0.1 M PB, pH 7.4. The brains were rapidly removed and postfixed in 4% PFA for 2 hour at RT. The brains were cryoprotected in 30% sucrose in 0.01 M PBS overnight at room temperature, frozen using powdered dry ice and stored at -20^{o}C until use. Twenty-five-µm-thick coronal sections were cut on a freezing microtome through the PVN and VLPAG or RMg into one-in-four series of sections.

Localization of virus injection sites

Series of sections containing the VLPAG or RMg were mounted onto glass slides and coverslipped with DAPI containing Vectashield mounting medium (Vector Laboratories Inc, Burlingame, CA, USA). The injection sites were detected based on the fluorescence of YFP.

Tissue preparation for examination of the innervation of TRH neurons by glycinergic neurons of the VLPAG and RMg

Sections of the PVN pre-treated as described above were incubated in a mixture of primary antisera: rabbit anti-GFP (1:10,000, ThermoFisher, Waltham, MA, USA) and sheep anti-tdTomato (1:80,000, generated in our laboratory) for 48h. After washing in PBS, sections were incubated in the cocktail of Alexa 488-conjucated donkey anti-rabbit IgG (1:250, Invitrogen) and Alexa 555-conjugated donkey anti-sheep IgG (1:500, Invitrogen, Carlsbad, CA, USA) for 2 h, mounted onto glass slides and coverslipped with Vectashield mounting medium.

Image analyzes of light microscopic preparations

Images of fluorescent preparations were taken using Zeiss LSM 780 confocal microscope (Zeiss Company, Jena, Germany) using line by line sequential scanning with laser excitation lines 490-553 nm for Alexa Fluor 488 and 566-697 nm for Alexa Fluor 555; beamsplitter/emission filters, MSB488/561 nm for Alexa Fluor 488 and Alexa Fluor 555. For 20x and 63x oil lenses, pinhole sizes were set to obtain optical slices of 2 and 0.7 μm thickness, respectively, and the series of optical sections were recorded with 0.6 μm Z steps.

Images were analyzed with Zen 2012 (Zeiss Company, Jena, Germany) and with Adobe Photoshop (Adobe System Inc., CA, USA).

Images of NiDAB stained preparations were captured with a Zeiss AxioImager M1 microscope using AxioCam MRc 5 digital camera (Zeiss Company, Jena, Germany) and AxioVision 4.6 software (Zeiss Company, Jena, Germany).

Specificity of the used antibodies

The specificity of rabbit anti-GlyT2 IgG (16), sheep anti-TRH IgG (17), guinea pig-GlyRa IgG (16) was previously described. The rabbit anti-RFP antibody (Rockland Immunochemicals, Limerick, PA, USA) and the rabbit anti-GFP serum (ThermoFisher, Waltham, MA, USA) did not generate any immunoreactivity on sections of wild type mice. The goat anti-CTB serum (List Biological Labs, Campbell, CA, USA) did not give any staining on sections of mice without tracer injection. The sheep antibody against tdTomato that was generated in our laboratory did not generate any staining on sections of wild type mice and the antibody did not crossreact with YFP.

In vitro Patch-Clamp Electrophysiology

Slice preparation for electrophysiological recordings

TRH-IRES-tdTomato mice (N=9) were deeply anaesthetized with isoflurane and decapitated. The brains were rapidly removed and immersed in ice-cold slicing solution (in mM: 87 NaCl, 2.5 KCl, 0.5 $CaCl_2$, 7 $MgCl_2$, 25 $NaHCO_3$, 25 D-glucose, 1.25 NaH_2PO_4, 75 sucrose) saturated with 95% O_2/5% CO_2. Coronal 250 µm slices were cut using a VT1200S vibratome (Leica Microsystems, Wetzlar, Germany), then the slices transferred into a holding chamber filled with artificial cerebrospinal fluid (aCSF; 36°C; in mM: 126 NaCl, 2.5 KCl, 26 $NaHCO_3$, 2 $CaCl_2$, 2 $MgCl_2$, 1.25 NaH_2PO_4, 10 glucose; pH 7.4; 280-300 mOsm/L). The slices were kept in holding solution for at least 1.5 hours and gradually brought to room temperature.

Chemicals used for electrophysiology

The chemicals for the intracellular and extracellular solutions, glycine and strychnine hemisulfate salt were purchased from Sigma-Aldrich (St. Louis, MO, USA). Tetrodotoxin (TTX), 6-Imino-3-(4-methoxyphenyl)-1(6*H*)-pyridazinebutanoic acid hydrobromide (Gabazine), and 4-Hydroxyquinoline-2-carboxylic acid sodium salt (kynurenic acid sodium salt, KYNA) were purchased from the Tocris Bioscience (Bristol, UK).

Data acquisition and analysis

The slices were transferred to a submersion type recording chamber containing aCSF at 32-33 °C and were perfused with aCSF at a rate of approximately 3 mL/min. TRH neurons were identified by the red fluorescence of the tdTomato under short epifluorescent illumination using an FN1 Microscope (Nikon, Tokio, Japan) equipped with 40x water-immersion objective with additional zoom (up to 2x) and Zyla CCD camera (ANDOR). Afterwards, the selected cell was studied under infrared differential interference contrast illumination. The patch pipettes (6-7 MΩ) were pulled from borosilicate capillaries (OD=1.5 mm thin wall, Garner Co, Maharashtra, India.) with a P-1000 horizontal puller (Sutter Instrument Co., Novato, CA, USA). The intracellular pipette solution used for current-clamp (I=0) electrophysiological recordings contained (in mM) 110 K-gluconate, 4 NaCl, 20 HEPES, 0.1 EGTA, 10 phosphocreatine di(tris) salt, 2 ATP, 0.3 GTP (pH 7.25; 280-300 mOsm/L). For sIPSC recording, the intracellular solution had the following composition: (in mM) 130 CsCl, 8 NaCl, 0.1 $CaCl_2$, 0.1 EGTA, 10 HEPES, 4 Mg-ATP, 0.3 Na_2-GTP, 5 Lidocaine N-ethyl bromide (pH 7.25; 280–300 mOsm/L). Recordings were performed with a Multiclamp 700B patch clamp amplifier, Digidata-1440A data acquisition system and pCLAMP 10.4 software (Molecular Devices). The headstage of the amplifier was fitted onto a Luigs&Neumann SM7 micromanipulator system. Whole-cell current-clamp recordings were filtered at 10 kHz using the built-in Bessel filter of the amplifier

and digitized at 10 kHz. Slow and fast capacitive components were automatically compensated for. The stability of the patch was checked by repetitively monitoring the access resistance during the experiment, and TRH neurons in which the series resistance changed >25% were excluded from the statistics. Liquid junction potential was 14.4 mV and not compensated.

Whole-cell patch clamp recording

After establishing a stable, whole-cell patch-clamp recording, a control period was recorded for 2-3 min that was followed by a drug treatment phase for 3-4 min. First, the effect of glycine (0.5 mM) was measured on the firing frequency of TRH neurons in the presence or absence of the glycine receptor inhibitor, strychnine (125 μM), in current-clamp mode (IC). Then, the voltage-dependent sodium channel inhibitor, TTX (1.2 mM), was added to the aCSF to prevent the potential indirect effects of glycine treatment, and the effect of glycine was also examined in the presence or absence of strychnine. The washout of the drugs restored the spiking frequency or the membrane potential of TRH neurons in all cases.

For glycinergic sIPSC recordings, cells were voltage clamped using a whole-cell clamp configuration at a holding potential of -63 mV, the average resting membrane potential of the TRH neurons. A control value was recorded for 2-3 min in the presence of Gabazine (3 μM) and KYNA (1 mM) to inhibit the effects of the GABAergic or glutamatergic inputs, followed by application of strychnine in the presence of Gabazine and KYNA for 3-4 min.

Statistical analysis of the data of electrophysiological recordings

Changes of spiking frequency, membrane potential and sIPSC recording were analyzed with Clampfit module of the pCLAMP 10.4 software (Molecular Devices, San José, CA, USA) and OriginPro 2015. Statistical analysis was performed using one-way analysis of variance (ANOVA) followed by the Bonferroni *post hoc* test to determine differences among treatment

groups in the current-clamp experiments, and the paired t-test was carried out in the voltage-clamp experiment. The number of studied cells is described in the results of each experiment. All data are reported as mean ± standard error of mean (SEM). The p value <0.05 was considered significant in all cases.

RESULTS

Colocalization of tdTomato-immunoreactivity and proTRH mRNA in the PVN of TRH-IRES-tdTomato mice

Drying results in fading of tdTomato's fluorescence, therefore its detection was performed by immunofluorescence in TRH-IRES-tdTomato mice. The distribution of tdTomato immunofluorescence (Fig. 1A) was found to be identical with the known distribution of TRH in the hypothalamus. *In situ* hybridization combined with immunofluorescence demonstrated a complete overlap between tdTomato-immunofluorescence and the *in situ* hybridization signal detecting the proTRH mRNA in the PVN. This demonstrated the selectivity and specificity of tdTomato expression in the generated *TRH-IRES-tdTomato* mice (Fig. 1B, C).

TRH neurons receive GLYT2-IR innervation in the PVN

GlyT2-IR axons were observed in close proximity to TRH-IR neurons in all subdivisions of the PVN where TRH neurons are located. By double-labeling immunofluorescence, large GLYT2-IR varicosities were observed on the surface of TRH-IR neurons (Fig 2). Quantification of the interaction of the two systems showed that GlyT2-IR axon varicosities established contacts with 53±2% of TRH neurons. An average of 1.9±0.1 GlyT2-IR contacts were found on the surface of the innervated TRH neurons. At the ultrastructural level, synaptic associations were observed between NiDAB-labeled, GlyT2-IR varicosities and TRH neurons labeled with silver intensified colloidal gold particles (Fig. 3). Both axo-somatic and axo-dendritic synapses were found between the two systems. All of the observed synaptic associations were of the symmetric type, indicating the inhibitory nature of these inputs.

TRH neurons express glycine receptors in the PVN

To understand whether glycine released from axon terminals can influence TRH neurons in the PVN, the glycine receptor content of TRH neurons was studied in TRH-IRES-tdTomato mice. Punctuate GLYR-immunoreactivity was observed in all TRH neurons in all subdivisions of the PVN (Fig. 4).

The ventrolateral PAG and the raphe magnus are the sources of the glycinergic input of TRH neurons in the PVN

As a first step, the retrograde tracer CTB was injected into the PVN of GlyT2::GFP mice to investigate the origins of the glycinergic input of the PVN. CTB injection sites localized well within the borders of the PVN (Fig. 5) were used for the colocalization of CTB-immunoreactivity and GFP, the latter labeling glycinergic neurons. Double-labeled PVN projecting glycinergic neurons were observed in only two regions of the brainstem: in the RMg and VLPAG (Fig. 5).

To determine whether the TRH neurons of the PVN receive glycinergic input from both of these brainstem nuclei, hChR2(H134R)-eYFP fusion protein was expressed specifically in the glycinergic neurons of the RMg or the VLPAG of TRH-IRES-tdTomato//GlyT2::Cre mice using AAV mediated gene transfer. The AAV injection site was centered within the RMg in 4 mice and in the VLPAG in 6 mice (Fig 6A, J). Axons of glycinergic neurons of RMg origin innervated symmetrically both parts of the PVN. While these axons densely innervated all parvocellular subdivisions of the PVN (Fig. 6 B-D), the magnocellular division of the PVN received less dense innervation. Glycinergic axons of VLPAG origin innervated primarily the ipsilateral side of the PVN, but sparse glycinergic axons were also observed on the contralateral side. Higher magnification images (Fig. 6E-I, N-Q) demonstrated that glycinergic axons originating from both the RMg and VLPAG contacted TRH neurons in all parvocellular

subdivisions of the PVN, demonstrating that the glycinergic input of TRH neurons originate from both the RMg and the VLPAG.

Glycine inhibits the firing of TRH neurons in the PVN

To understand the role of glycine in the regulation of TRH neurons, the effects of this amino acid transmitter was studied on the membrane potential and firing of TRH neurons in the mid level of PVN of TRH-IRES-tdTomato mice, where the hypophysiotropic TRH neurons are enriched (13). Application of glycine markedly decreased the membrane potential (-14.23±2.55 mV; n=6, P<0.001; Fig. 7) and completely blocked the firing (control: 3.15±0.52 Hz *vs.* glycine: 0.08±0.08 Hz, n=6, P<0.001; Fig. 7) of TRH neurons. Co-application of strychnine completely prevented the glycine-induced changes of the membrane potential (0.16±1.65 mV, P=1 *vs.* control and P<0.001 *vs.* glycine, n=6; Fig. 7) and the firing rate (0.38±0.54 Hz, P=1 *vs.* control and P<0.001 *vs*. glycine, n=6; Fig. 7) of TRH neurons.

To understand whether the inhibitory effect of glycine is exerted directly on the TRH neurons, the effect of glycine was also studied in the absence of neuronal inputs in TTX (1.2 mM) treated slides. Application of glycine caused an approximately 6 mV hyperpolarization of TRH neurons (control: -63.20±0.94 mV *vs*. Gly: -69.84±0.65 mV, n=5, P=0.0011; Fig. 7 D, E) even in the presence of TTX. Application of strychnine abolished this effect of glycine (-64.11±1.58 mV, n=5; Fig. 7 D, E).

TRH neurons receive spontaneous inputs from glycinergic terminals

To demonstrate the involvement of the glycinergic inputs in the regulation of TRH neurons of the PVN, the spontaneous glycinergic currents of these cells were studied in TRH-IRES-tdTomato mice. Glycinergic sIPSCs were isolated by simultaneous inhibition of the glutamatergic and GABAergic inputs with a mixture of KYNA and Gabazine. Despite the

presence of these inhibitors, sIPSCs were observed in 62.5% of TRH neurons. The frequency of these sIPSCs was 0.824±0.19 Hz (Fig. 8). Strychnine markedly decreased the frequency of these sIPSCs (0.12±0.04 Hz, n=5, P=0.038; Fig. 8) suggesting that glycinergic synaptic inputs inhibit a population of TRH neurons. In 37.5% of the studied TRH neurons (n=3), the frequency of sIPSCs was only 0.080±0.014 Hz after inhibition of GABAergic and glutamatergic currents cells with *vs.* without glycinergic sIPSC: P=0.028). Strychnine had no effect on the sIPSC frequency of these cells (0.080±0.045 Hz; P=0.963).

Discussion

An important function of the HPT axis is to maintain stable thyroid hormone levels in the circulation under normal conditions and thus, to provide a continuous supply of thyroid hormones for tissues (8). This function is primarily controlled by the negative feedback effect of thyroid hormones on hypophysiotropic TRH neurons and pituitary thyrotrophs (8). Under certain conditions, such as fasting, infection or cold exposure, however, the activity of the HPT axis is altered by neuronal inputs or by the activity of tanycytes (8). Peptidergic inputs originating from the arcuate nucleus are known to mediate the effects of fasting and leptin treatment on the hypophysiotropic TRH neurons (8), while adrenergic innervation stimulates the hypophysiotropic TRH neurons during cold exposure (20). Our laboratories described that the TRH neurons of the PVN also receive inputs from neurons utilizing classical neurotransmitters such as GABA and glutamate (21, 22). Since glycinergic axons are also present in the PVN (3), we investigated whether TRH neurons are also controlled by glycine to regulate the thyroid axis.

To facilitate these studies, we generated a novel *knock in* mouse model expressing tdTomato specifically in TRH-producing cells using the CRISPR/Cas9 technology. By combined immunocytochemistry and *in situ* hybridization, we showed that there is a complete overlap of tdTomato protein and the proTRH mRNA in the PVN of these mice, indicating that the TRH-IRES-tdTomato mouse line allows specific identification of the TRH neurons. This new mouse line also enabled us to study the electrophysiology of TRH neurons and identify the TRH neurons in morphological studies without the use of colchicine, an axonal transport inhibitor.

Our presented data demonstrate that glycinergic neurons innervate approximately half of the TRH neurons in the PVN, establishing symmetric type synapsis suggesting the inhibitory nature of these connections (23, 24). In addition, we show that the vast majority of TRH neurons express glycine receptors. In agreement with these morphological findings, exogenous glycine

inhibited all TRH neurons studied in the PVN. Namely, glycine treatment markedly hyperpolarized TRH neurons and almost completely abolished the firing of these cells.

While approximately half of the TRH neurons received glycinergic innervation, almost all TRH neurons in the PVN contained glycine receptors and responded to glycine treatment. This discrepancy raised the question whether the sensitivity of the immunocytochemical method was insufficient to detect all of the glycinergic input to TRH neurons, or whether the glycine receptors of these neurons have other roles in addition to the detection of synaptically-released glycine. To address this question, we studied the glycinergic sIPSCs of TRH neurons.

After inhibition of glutamatergic and GABAergic currents, sIPSCs were still observed in approximately 60% of TRH neurons in the PVN. Administration of strychnine almost completely blocked the sIPSCs, demonstrating that endogenous glycine released from neuronal terminals exerts an inhibitory effect on TRH neurons in the PVN. However, glycinergic sIPSCs were not observed in approximately 40% of TRH neurons in the PVN. These data indicate that extrasynaptic glycine receptors are also involved in the regulation of TRH neurons.

In addition to glycine, taurine is also a known ligand of glycine receptors (25). In the supraoptic nucleus (SON), Deleuze et al (25) showed that the neurons express glycine receptors, but do not receive functional glycinergic synapses. Furthermore, they observed that the glycine receptor expressing cells are contacted by taurine containing astrocytes (22, 25). Based on these observations, they suggested that the ligand of glycine receptor in the SON is taurine, released from astrocytes (25). Thus, it seems feasible that TRH neurons in the PVN may also be regulated by both glycine, released from neuronal inputs, and by taurine, secreted by astrocytes and will require further investigation.

Although, glycinergic neurons are present in most parts of the brainstem, the origin of the glycinergic input to TRH neurons in the PVN is restricted to two, brainstem nuclei, the VLPAG and RMg. The role of these nuclei in the regulation of the TRH neurons and the HPT axis is

currently unknown. Published data, however, indicate that some of the conditions known to inhibit the HPT axis, such as the administration of bacterial lipopolysaccharide (LPS), a model of infection or different stressors (8), induces neuronal activation in the VLPAG and RMg (10, 25-30). Thus, further studies are needed to determine whether projections from glycinergic neurons in these two, brainstem regions to TRH neurons in the PVN have a role in the mediation of the stress and LPS-induced inhibition of the hypophysiotropic TRH neurons and the HPT axis.

Glycinergic inputs of TRH neurons found not only in the mid level of the PVN, where the hypophysiotropic TRH neurons are concentrated (13), but also in other regions of the PVN, like in the anterior parvocellular subdivision, where the TRH neurons have no hypophysiotropic function (13). Therefore, our data indicate that glycine regulates both hypophysiotropic and non-hypophysiotropic populations of the TRH neurons in the PVN. Currently very little information is available about the function of non-hypophysiotropic TRH neurons of the PVN. The TRH neurons residing in the anterior parvocellular subdivision of the PVN were, however, shown to project to energy homeostasis-related areas, like the arcuate and ventromedial nuclei {Wittmann, 2009 #22}, thus it is feasible that the glycinergic neurons regulate the energy homeostasis via the non-hypophysiotropic TRH neurons.

In summary, these data demonstrate that TRH neurons in the PVN receive a functional, glycinergic input from the VLPAG and the RMg that exert an inhibitory effect on the TRH neurons, indicating that the glycinergic system may have an important role in the central regulation of the HPT axis. However, as not all TRH neurons in the PVN are innervated by glycinergic inputs yet responsive to glycine *in vitro*, we hypothesize that glial release of glycine or taurine, or yet another glycine receptor agonist, may also influence TRH neurons *via* glial-neuronal interactions.

Acknowledgments

This work was supported by Grants from the Hungarian Science Foundation (OTKA K124767), the Hungarian National Brain Research Program (2017-1.2.1-NKP-2017-00002) and EU H2020 THYRAGE no. 666869. The authors are very grateful to Dr. Hanns Ulrich Zeilhofer (University of Zurich, Zurich, Switzerland) for the kind gift of GLYT2::GFP and GLYT2::Cre mice.

Author Disclosure Statement:

The authors declare no competing financial interests.

Refrences

1. Hernandes MS, Troncone LR 2009 Glycine as a neurotransmitter in the forebrain: a short review. Journal of neural transmission (Vienna, Austria : 1996) **116**:1551-1560.
2. Zafra F, Gomeza J, Olivares L, Aragon C, Gimenez C 1995 Regional distribution and developmental variation of the glycine transporters GLYT1 and GLYT2 in the rat CNS. The European journal of neuroscience **7**:1342-1352.
3. Zeilhofer HU, Studler B, Arabadzisz D, Schweizer C, Ahmadi S, Layh B, Bosl MR, Fritschy JM 2005 Glycinergic neurons expressing enhanced green fluorescent protein in bacterial artificial chromosome transgenic mice. The Journal of comparative neurology **482**:123-141.
4. Poyatos I, Ponce J, Aragon C, Gimenez C, Zafra F 1997 The glycine transporter GLYT2 is a reliable marker for glycine-immunoreactive neurons. Brain research Molecular brain research **49**:63-70.
5. Zafra F, Gimenez C 2008 Glycine transporters and synaptic function. IUBMB life **60**:810-817.
6. Dutertre S, Becker CM, Betz H 2012 Inhibitory glycine receptors: an update. The Journal of biological chemistry **287**:40216-40223.
7. Johnson JW, Ascher P 1987 Glycine potentiates the NMDA response in cultured mouse brain neurons. Nature **325**:529-531.
8. Fekete C, Lechan RM 2014 Central regulation of hypothalamic-pituitary-thyroid axis under physiological and pathophysiological conditions. Endocrine reviews **35**:159-194.
9. Vavra V, Farkas E, Capraru O, Watanabe M, Fekete C, Bains JS 2014 Evidence for functional glycinergic transmission in the paraventricular nucleus of the hypothalamus Annual Meeting of the Society for Neuroscience, Washington, 124.101.
10. Foster E, Wildner H, Tudeau L, Haueter S, Ralvenius WT, Jegen M, Johannssen H, Hosli L, Haenraets K, Ghanem A, Conzelmann KK, Bosl M, Zeilhofer HU 2015 Targeted ablation, silencing, and activation establish glycinergic dorsal horn neurons as key components of a spinal gate for pain and itch. Neuron **85**:1289-1304.
11. Singh P, Schimenti JC, Bolcun-Filas E 2015 A mouse geneticist's practical guide to CRISPR applications. Genetics **199**:1-15.
12. Albagli-Curiel O, Lecluse Y, Pognonec P, Boulukos KE, Martin P 2007 A new generation of pPRIG-based retroviral vectors. BMC biotechnology **7**:85.
13. Kadar A, Sanchez E, Wittmann G, Singru PS, Fuzesi T, Marsili A, Larsen PR, Liposits Z, Lechan RM, Fekete C 2010 Distribution of hypophysiotropic thyrotropin-releasing hormone (TRH)-synthesizing neurons in the hypothalamic paraventricular nucleus of the mouse. The Journal of comparative neurology **518**:3948-3961.
14. Fekete C, Mihaly E, Luo LG, Kelly J, Clausen JT, Mao Q, Rand WM, Moss LG, Kuhar M, Emerson CH, Jackson IM, Lechan RM 2000 Association of cocaine- and amphetamine-regulated transcript-immunoreactive elements with thyrotropin-releasing hormone-synthesizing neurons in the hypothalamic paraventricular nucleus and its role in the regulation of the hypothalamic-pituitary-thyroid axis during fasting. The Journal of neuroscience : the official journal of the Society for Neuroscience **20**:9224-9234.
15. Wittmann G, Fuzesi T, Liposits Z, Lechan RM, Fekete C 2009 Distribution and axonal projections of neurons coexpressing thyrotropin-releasing hormone and urocortin 3 in the rat brain. J Comp Neurol **517**:825-840.
16. Hondo M, Furutani N, Yamasaki M, Watanabe M, Sakurai T 2011 Orexin neurons receive glycinergic innervations. PloS one **6**:e25076.
17. Wittmann G, Fuzesi T, Liposits Z, Lechan RM, Fekete C 2009 Distribution and axonal projections of neurons coexpressing thyrotropin-releasing hormone and urocortin 3 in the rat brain. The Journal of comparative neurology **517**:825-840.
18. Branchereau P, Van Bockstaele EJ, Chan J, Pickel VM 1995 Ultrastructural characterization of neurons recorded intracellularly in vivo and injected with lucifer yellow: advantages of immunogold-silver vs. immunoperoxidase labeling. Microscopy research and technique **30**:427-436.

19. Paxinos G, Watson C 1998 The Rat Brain in Stereotaxic Coordinates. Academic Press, San Diego, CA.

20. Wittmann G 2008 Regulation of hypophysiotrophic corticotrophin-releasing hormone- and thyrotrophin-releasing hormone-synthesising neurones by brainstem catecholaminergic neurones. Journal of neuroendocrinology **20**:952-960.

21. Fekete C, Wittmann G, Liposits Z, Lechan RM 2002 GABA-ergic innervation of thyrotropin-releasing hormone-synthesizing neurons in the hypothalamic paraventricular nucleus of the rat. Brain research **957**:251-258.

22. Wittmann G, Lechan RM, Liposits Z, Fekete C 2005 Glutamatergic innervation of corticotropin-releasing hormone- and thyrotropin-releasing hormone-synthesizing neurons in the hypothalamic paraventricular nucleus of the rat. Brain research **1039**:53-62.

23. Peters A, Palay SL, deF Webster H 1991 The fine structure of the nervous system. Neurons and their supporting cells. Third Edition ed. Oxford University Press, Oxford.

24. Somogyi P, Soltesz I 1986 Immunogold demonstration of GABA in synaptic terminals of intracellularly recorded, horseradish peroxidase-filled basket cells and clutch cells in the cat's visual cortex. Neuroscience **19**:1051-1065.

25. Deleuze C, Alonso G, Lefevre IA, Duvoid-Guillou A, Hussy N 2005 Extrasynaptic localization of glycine receptors in the rat supraoptic nucleus: further evidence for their involvement in glia-to-neuron communication. Neuroscience **133**:175-183.

26. Furlong TM, McDowall LM, Horiuchi J, Polson JW, Dampney RA 2014 The effect of air puff stress on c-Fos expression in rat hypothalamus and brainstem: central circuitry mediating sympathoexcitation and baroreflex resetting. The European journal of neuroscience **39**:1429-1438.

27. Devall AJ, Lovick TA 2010 Differential activation of the periaqueductal gray by mild anxiogenic stress at different stages of the estrous cycle in female rats. Neuropsychopharmacology : official publication of the American College of Neuropsychopharmacology **35**:1174-1185.

28. Lino-de-Oliveira C, de Oliveira RM, Padua Carobrez A, de Lima TC, del Bel EA, Guimaraes FS 2006 Antidepressant treatment reduces Fos-like immunoreactivity induced by swim stress in different columns of the periaqueductal gray matter. Brain research bulletin **70**:414-421.

29. Lino-de-Oliveira C, Sales AJ, Del Bel EA, Silveira MC, Guimaraes FS 2001 Effects of acute and chronic fluoxetine treatments on restraint stress-induced Fos expression. Brain research bulletin **55**:747-754.

30. Imbe H, Murakami S, Okamoto K, Iwai-Liao Y, Senba E 2004 The effects of acute and chronic restraint stress on activation of ERK in the rostral ventromedial medulla and locus coeruleus. Pain **112**:361-371.

Figures

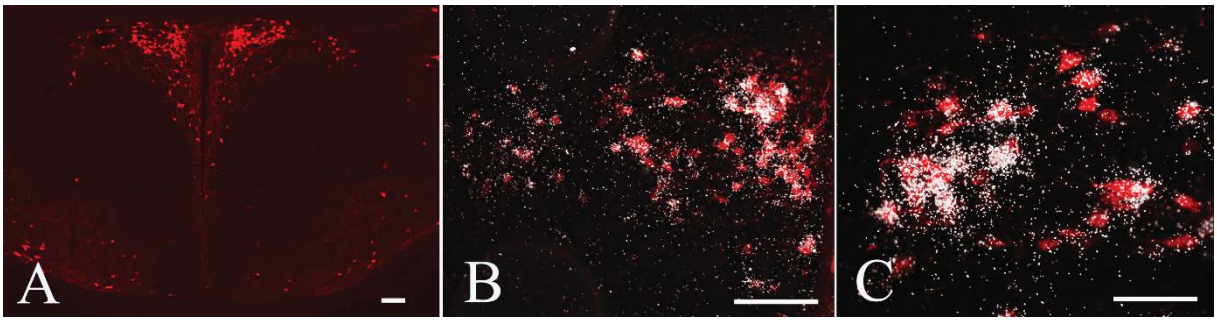

Figure 1. Characterization of the TRH-IRES-tdTomato mice. Low magnification image (A) illustrates that the distribution of the tdTomato-immunoreactivity in the TRH-IRES-tsTomato mice is identical with the known distribution of TRH in the hypothalamus. Double-labeling combined in situ hybridization and immunofluorescence (B) demonstrate the complete overlap of tdTomato (red) and proTRH mRNA (silver grain) in the PVN. Higher magnification image (C) shows the colocalization of the two signals in the PVN. Scale bars on A and B = 100µm, on C = 50µm.

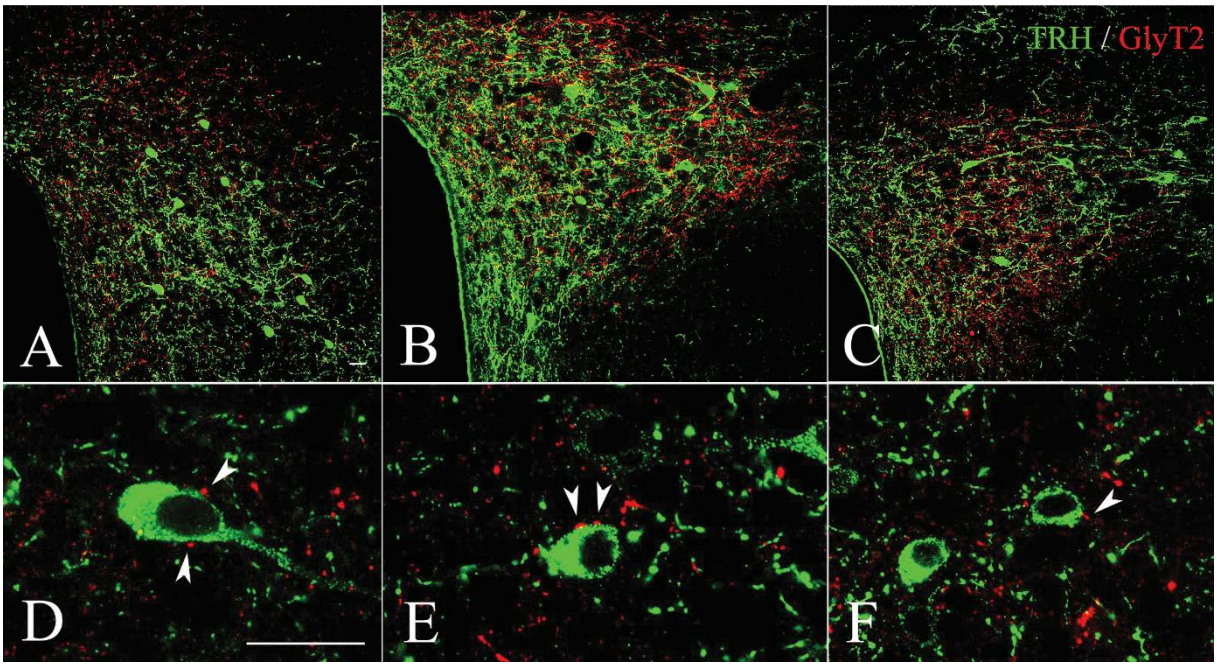

Figure 2. Relationship of GLYT2-IR axons and TRH-IR neurons in the PVN of CD1 mice. GlyT2-IR (red) axons were observed in close proximity of the TRH-IR (green) neurons in all subdivisions of the PVN. A-C figures show the relationship of GLYT2-IR axons and TRH neurons in the anterior (A), mid (B) and posterior (C) levels of the PVN. Higher magnification images illustrate the GLYT2-IR boutons (arrowheads) on the surface of TRH neurons in the anterior (D), mid (E) and posterior (F) levels of the PVN. Scale bars= 20 µm, Scale bar on A corresponds to A-C, Scale bar on D corresponds to D-F.

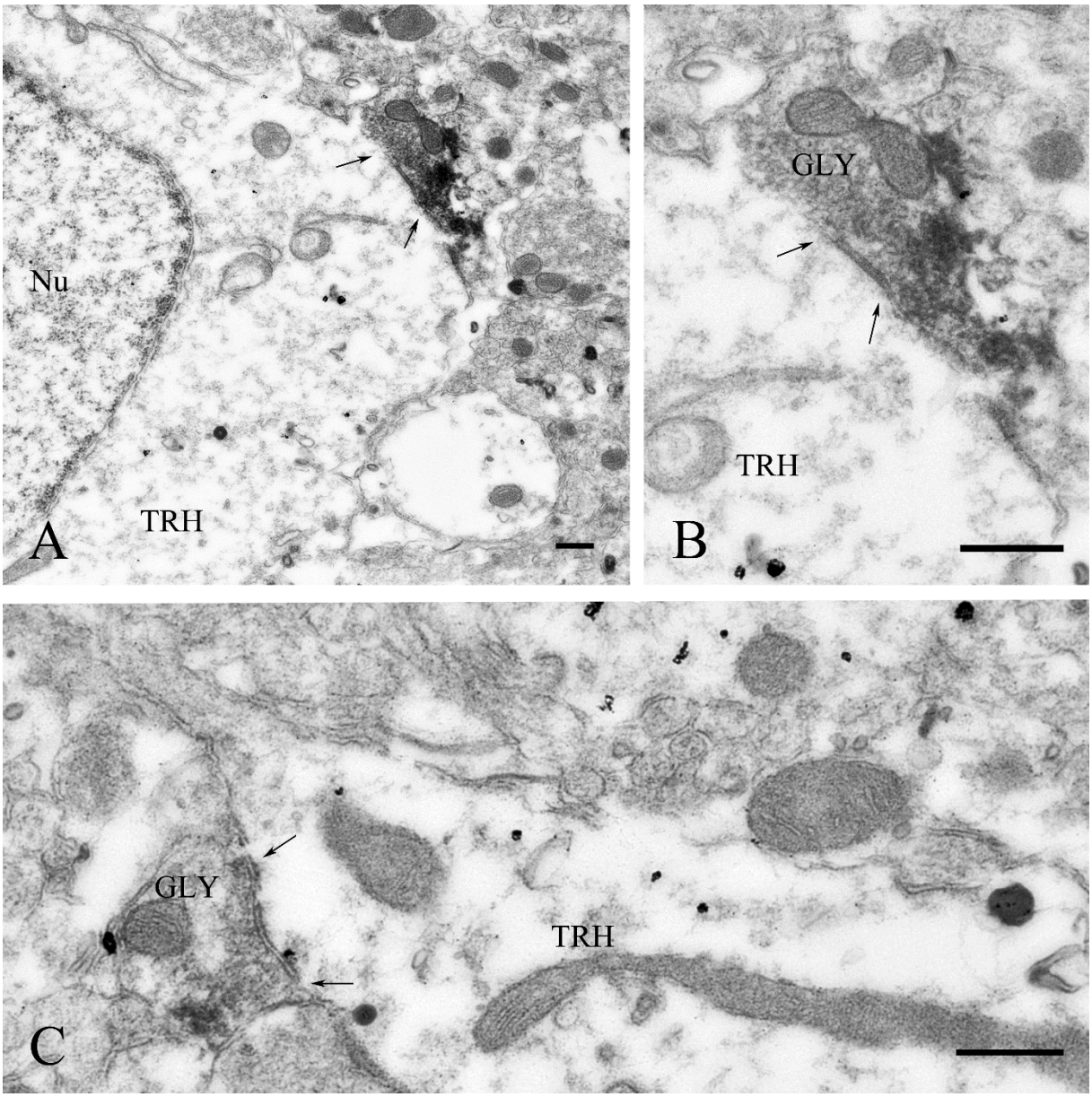

Figure 3. GLYT2-IR varicosities establish symmetric type synapses on TRH neurons in the PVN of CD1 mice. At the ultrastructural level, synaptic associations were observed between NiDAB labeled GlyT2-IR varicosities and TRH neurons labeled with silver intensified colloidal gold particles. Both axo-somatic (A, and in higher magnification on B), and axo-dendritic synapses (C) were found between the two systems. These synaptic associations were of symmetric type indicating the inhibitory nature of these inputs. Scale bar: 200 nm.

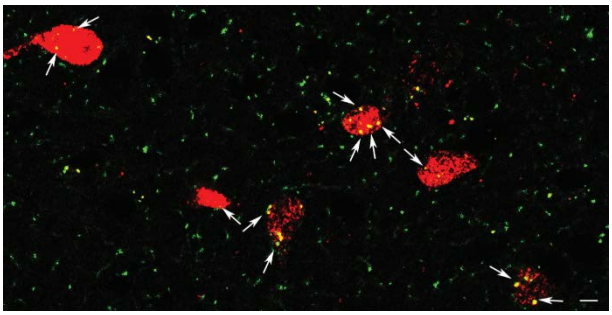

Figure 4. Presence of glycine receptor-immunoreactivity in the TRH neurons in the PVN of TRH-IRES-tdTomato mice. Punctuate glycine receptor-immunoreactivity (green) is present in all TRH neurons (red) studied. Scale bar = 5µm

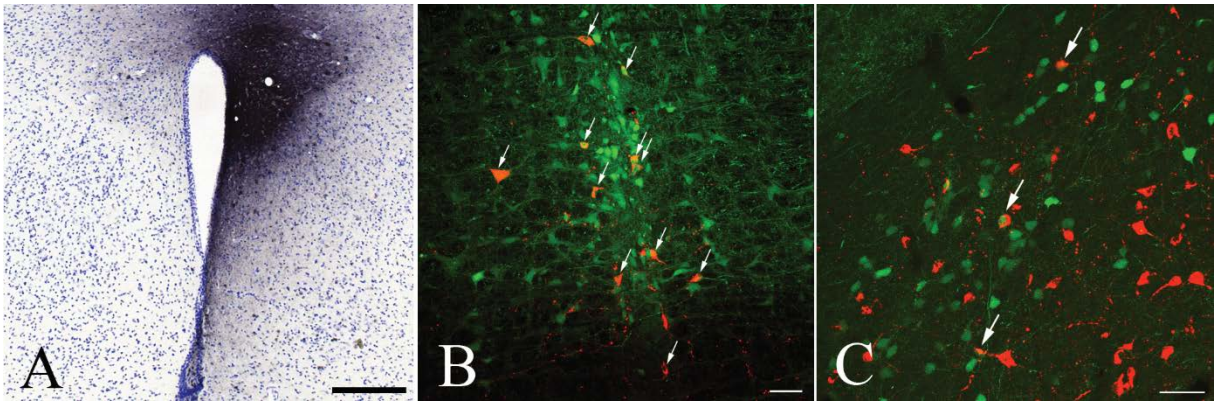

Figure 5. Origin of the glycinergic input of the PVN of GLYT2::GFP mice. (A) illustrates a representative CTB injection site. The CTB immunoreactivity was visualized using NiDAB chromogen. Nissl staining was used to facilitate the identification of the borders of the PVN. Immunofluorescent preparations demonstrate the presence of the PVN projecting (red, CTB-immunoreactive) glycinergic neurons (green, GLYT2-GFP) in the RMg (B) and VLPAG (C). Arrows point to the double-labeled neurons. Scale bar on A = 200µm, on B and C = 50µm.

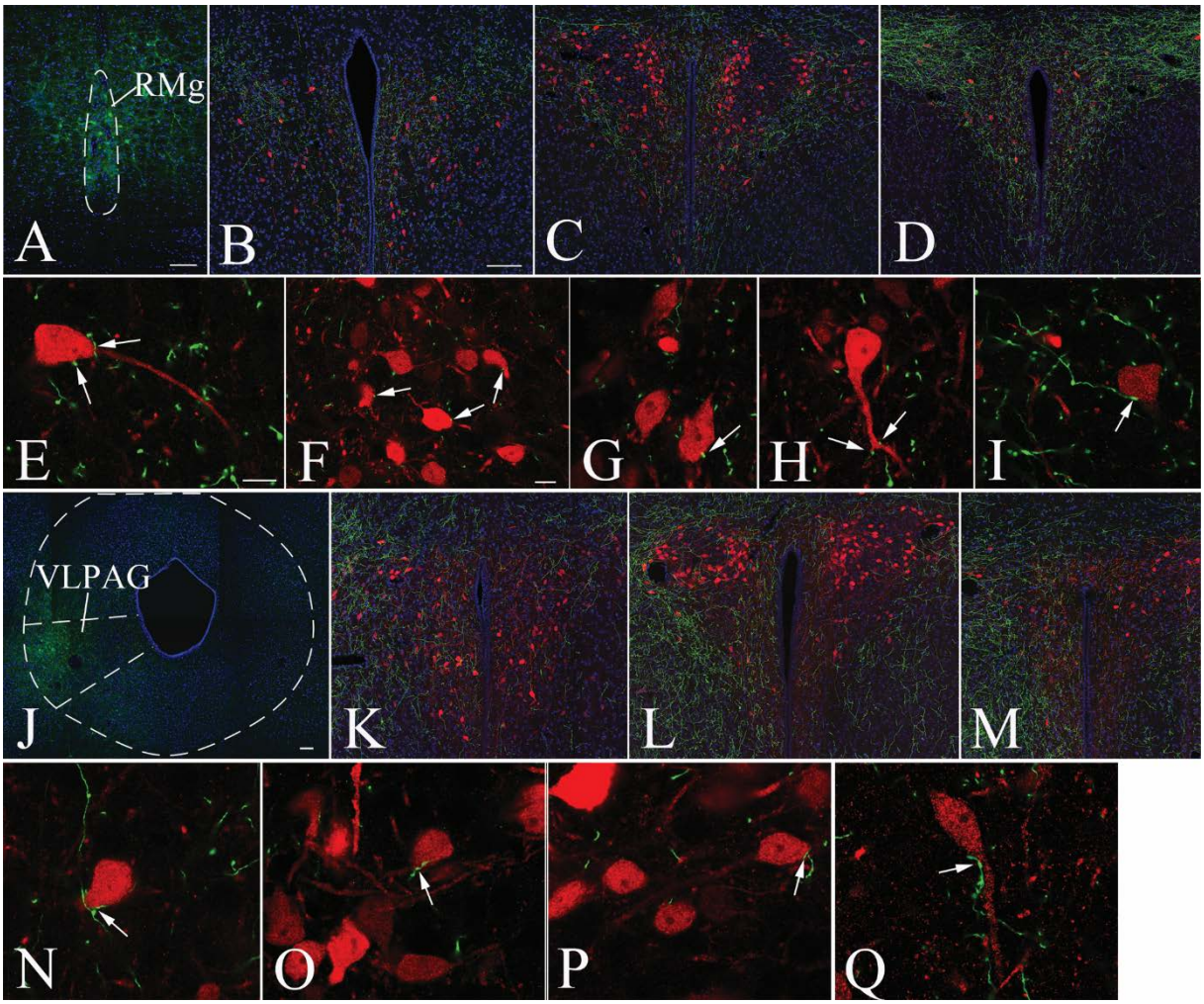

Figure 6. Involvement of the glycinergic neurons of the RMg and VLPAG in the innervation of the TRH neurons in the PVN of TRH-IRES-tdTomato//GlyT2::Cre mice. A representative image (A) illustrates the AAV mediated expression of hChR2(H134R)-eYFP fusion protein (green) in RMg gylcinergic neurons of TRH-IRES-tdTOMATO//GlyT2-Cre mice. Low magnification images illustrate the distribution of the glycinergic axons (green) in the parvocellular subdivisions of the PVN of originating from the RMg and their relationship to the TRH neurons (red) in the anterior (B), mid (C) and (D) posterior levels of the PVN. While the glycinergic axons originating from the RMg densely innervate the parvocellular subdivisions on both sides of the hypothalamus, only low density of axons are observed in the magnocellular subdivision (C). High magnification images demonstrate the juxtaposition of glycinergic axons

of RMg origin to TRH neurons in the anterior (E), mid (F-H) and posterior (I) levels of the PVN.

A representative image (J) illustrates the AAV-mediated expression of hChR2(H134R)-eYFP fusion protein in glycinergic neurons of VLPAG of TRH-IRES-tdTOMATO//GlyT2-Cre mice. Low magnification images illustrate the distribution of the glycinergic axons of VLPAG origin in the parvocellular subdivision of the PVN and their relationship to TRH neurons (red) at the anterior (K), mid (L) and (M) posterior levels of the PVN. The gylcinergic input of VLPAG origin primarily innervates the ipsilateral side, but axons can also be observed on the contralateral side. High magnification images demonstrate the juxtaposition of the glycinergic axons of VLPAG origin to TRH neurons at the anterior (N), mid (O,P) and posterior (Q) levels of the PVN. DAPI counterstaining (blue) was used to facilitate the identification of brain regions (A-D, J-M). Arrows point to glycinergic axons juxtaposed to TRH neurons. Scale bar on A and J = 100 µm; on B = 100 µm corresponds to B-D and K-L; on E = 10 µm corresponds to E, G-I and N-Q; on F = 10 µm.

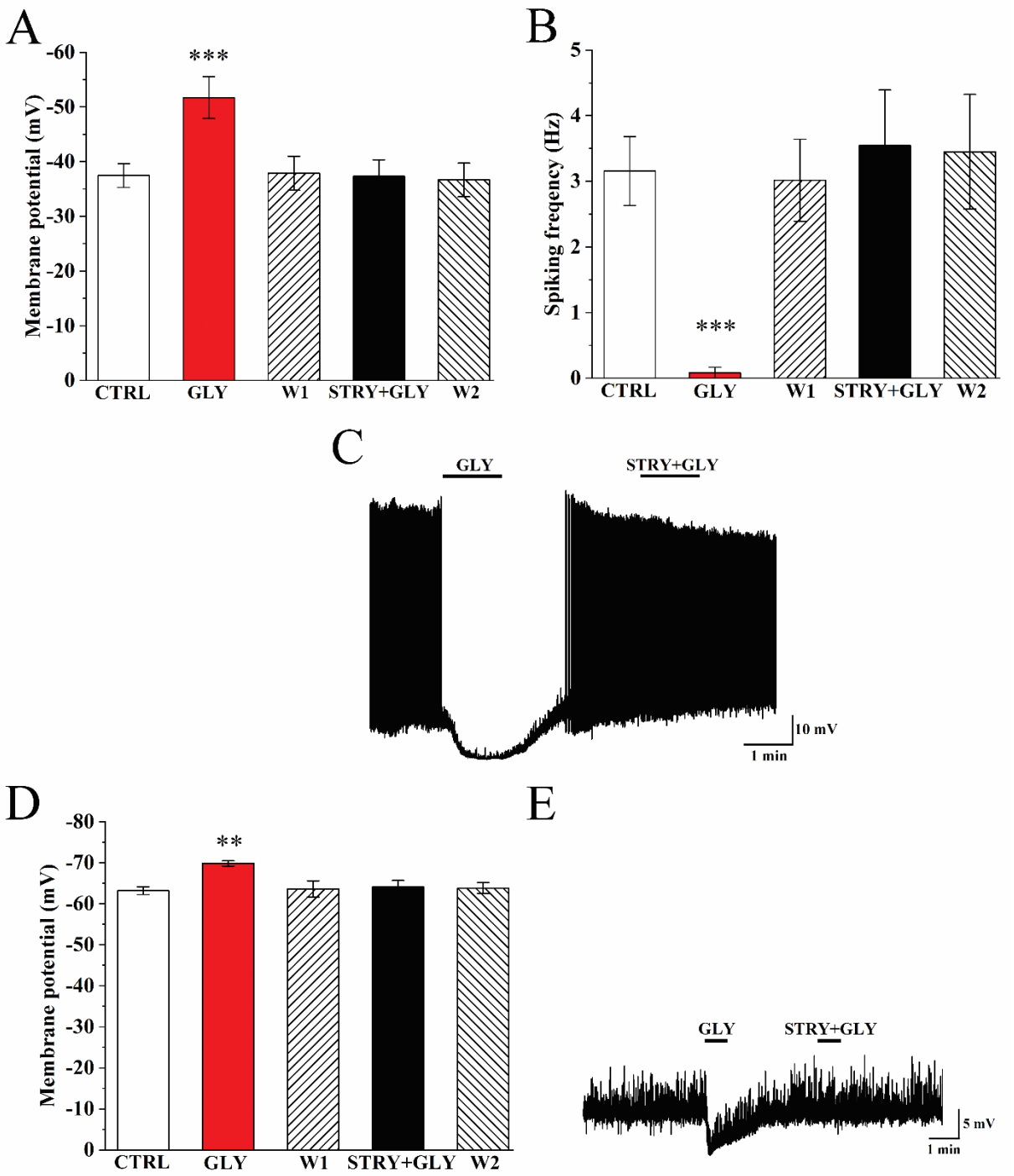

752

753 **Figure 7.** Effect of glycine on the membrane potential and the spiking frequency of TRH
754 neurons. Bar graphs show changes of membrane potential (A) and the firing frequency (B) of
755 TRH neurons in a response to glycine in the presence or absence of the glycine receptor
756 inhibitor, strychnine. Glycine, alone, decreased the membrane potential and completely
757 inhibited the firing of TRH neurons. Strychnine prevented these effects of glycine.
758 Representative trace (C) illustrates the effects of glycine on the membrane potential and firing

rate of a TRH neuron, and the absence of the glycine-induced changes when strychnine is co-administered. To understand whether this effect of glycine is exerted directly on the TRH neurons, the effect of glycine was studied in the presence of TTX. Bar graph (D) shows the change of the membrane potential of TRH neurons in the presence of TTX in a response to glycine in the presence or absence of the glycine receptor inhibitor, strychnine. A representative trace is shown on (E). Bath application of glycine depolarized the TRH neurons in the presence of TTX. Strychnine completely prevented this effect of glycine. ** or *** labels significant difference ($P<0.01$ or $P<0.001$, respectively) based on repeated measure ANOVA followed by Bonferroni *post hoc* test. Data are expressed as mean ± SEM. Abbreviations: control – CTRL, glycine – GLY, washout – W and strychnine – STRY.

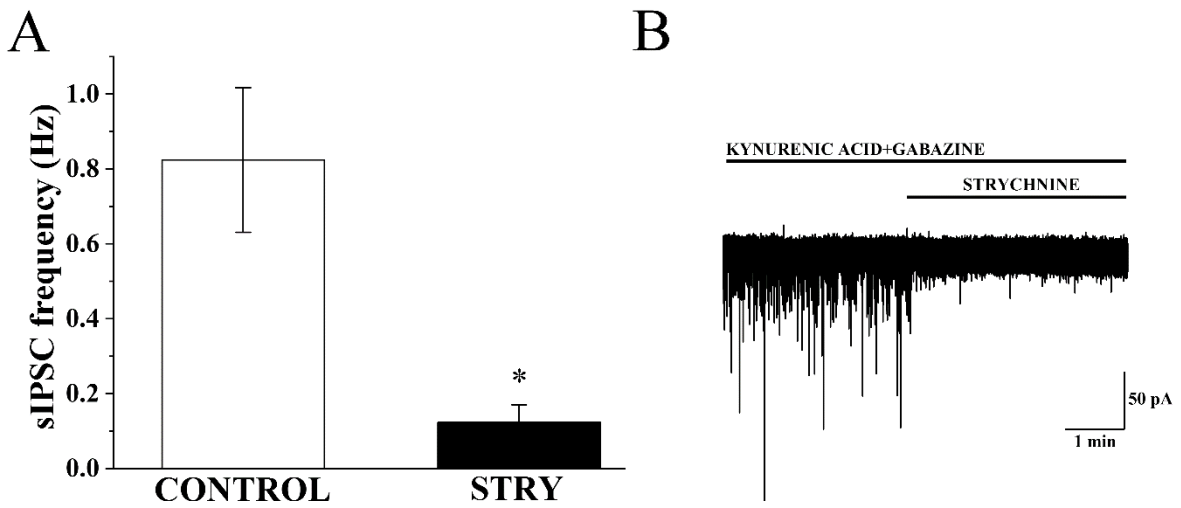

Figure 8. Examination of glycinergic spontaneous inhibitory postsynaptic currents on TRH neurons. Bar graph (A) shows the average frequency of the sIPSCs of TRH neurons in the presence of glutamate and GABA receptor inhibitors and the effect of strychnine on the frequency of these currents. A representative trace illustrates that application of strychnine markedly inhibited the sIPSCs of TRH neurons in the presence of KYNA and gabazine. * presents significant difference ($P<0.05$) based on the paired sample t-test. Data are expressed as mean ± SEM. Abbreviations: strychnine – STRY.